Optics and Spectroscopy, 2024, Vol. 132, No. 11

01

Relativistic calculations of potential energies of low-lying electronic states and transition dipole moments of the OH radical

© *D.P. Usov*[1], *N.K. Dulaev*[1], *A.V. Stolyarov*[2], *Y.S. Kozhedub*[1], *I.I. Tupitsyn*[1], *V.M. Shabaev*[1,3]

[1] St. Petersburg State University,
St. Petersburg, Russia
[2] Department of Chemistry, Lomonosov Moscow State University,
Moscow, Russia
[3] Petersburg Nuclear Physics Institue, National Research Center „Kurchatov Institute“,
Gatchina, Russia

e-mail: st054876@student.spbu.ru

Received November 15, 2024
Revised November 15, 2024
Accepted November 25, 2024

Relativistic calculation of molecular properties of low-lying electronic states of the OH radical has been performed using various *ab initio* quantum chemical methods. This study yielded potential energy curves for electronic states in a wide range of internuclear distances converging toward the three lowest dissociation limits of the OH radical. The dependencies of relativistic corrections, Gaunt contribution, spin-orbit splitting and quantum-electrodynamic correction to the total energy on the internuclear distance have been established for the ground state. Additionally, the dipole moment curve of the ground state was calculated over a wide range of internuclear distances. For electronic states asymptotically approaching the lowest dissociation limit, the transition dipole moment curves were computed for transitions to the ground state, including both spin-allowed and spin-forbidden transitions. The results obtained are important for investigating the processes of hydroxyl molecule formation in the interstellar medium.

Keywords: relativistic effects, correlation effects, quantum-electrodynamic corrections, hydroxyl OH.

DOI: 10.61011/EOS.2024.11.60317.7347-24

Introduction

The study of the free hydroxyl radical (OH molecule) is important in various fields of modern molecular physics and physical chemistry. Intense vibrational-rotational transitions in the ground $X^2\Pi$ electronic state of the OH radical are the main source of the Earth's own atmospheric radiation [1–3]. The hydroxyl is actively involved in chemical processes affecting the density of the ozone layer [4,5]. As a strong oxidizing agent, the OH molecule plays an essential role in combustion mechanisms [6]. The OH molecule is also an important component of a variety of astrochemical transformations. Analyzing the OH spectral lines makes it possible to determine the oxygen content of stars, including the Sun [7–9]. The hydroxyl molecule was one of the first to be detected in the interstellar medium [10,11], as well as in the atmospheres of exoplanets [12].

A large number of both experimental and theoretical works on the structure and dynamics of the OH molecule in a wide range of its electron-vibrational-rotational excitation have been accumulated in the literature. The most complete data are available for the ground $X^2\Pi$ and the first excited $A^2\Sigma^+$ doublet states [13–22]. Also, ab initio calculations of the energies of the following excited doublet and quartet states [23–32], converging to the first three dissociation limits of the molecule, are available (Fig. 1). In addition to the potential energy curves, the dipole moments of various states of the hydroxyl molecule have been investigated in Refs. [14–19,25,28,29]. In the overwhelming majority of published studies, either the fully nonrelativistic or scalar-relativistic approximation was used, and the electronic correlations were taken into account within the framework of the Multi-Reference Configuration Interaction (MRCI) method.

To accurately describe the spectroscopically measurable intensities of optical transitions and the radiative lifetimes of the OH molecule over a wide range of vibrational and rotational quantum numbers, it is essential to have detailed knowledge of the dipole moment curves of the electronic states, as well as the transition dipole moment functions (including spin-forbidden transitions) over an extended range of internuclear distances. Previous studies [16,19,22,25] have investigated the permanent dipole moment of the ground electronic state and the dipole moment of the most frequently observed emission transition, $A^2\Sigma^+ \to X^2\Pi$. In addition, Ref. [29] presents spin-allowed dipole moments for transitions between the ground state and several of the most significant low-lying electronic terms of the OH molecule.

For realistic modeling of predissociation (nonradiative) and photodissociation (optical) properties of electronically excited states of the OH molecule, high-precision information on the potential energy curves of repulsive (or more precisely, weakly bound) doublet and quartet states converging to the main dissociation limit [32], is extremely important (see Fig. 1). These so-called „dark“ states typically do not participate directly in the majority of observed optical transitions due to spin-forbidden selection rules. Consequently, empirical information regarding these states can generally only be inferred indirectly, which makes the results of direct non-empirical electronic structure calculations particularly valuable. In addition, these repulsive „dark“ states are responsible for the processes of radiation-induced association and cooling that occur on a cosmological time scale during the binary collision of isolated oxygen and hydrogen atoms in a highly rare-field interstellar medium:

$$\mathrm{O} + \mathrm{H} \rightarrow \mathrm{OH} + h\nu$$

In order to correctly estimate the rates of these extremely slow processes, we also need dipole moment curves of the corresponding spin-forbidden transitions, which can be adequately obtained only in the framework of strict relativistic methods of quantum mechanics.

Thus, this study aimed to perform systematic relativistic calculations of energies, permanent dipole moments, and dipole moment transitions of the ground state and a number of low-lying excited electronic states of the OH molecule over a wide range of internuclear distances. For high-precision calculations of the ground state in the region of the potential energy minimum, the single-reference coupled cluster method, which accurately accounts for excitations up to and including the third order (CCSDT), was used. Based on the experimental value of the spin-orbit splitting in the spectrum of the oxygen atom in the ground state $\mathrm{O}(^3P)$, one should expect that the averaged value of the spin-orbit effect in the hydroxyl molecule should be at the level of $100-150\,\mathrm{cm}^{-1}$, which is comparable to the uncertainty of the calculation of the correlation energy by the CCSDT method and makes expensive relativistic calculations quite justified. To calculate the potential energy and dipole moment curves of the ground and excited states, as well as spin-resolved and spin-forbidden dipole moments of transitions, we used the MRCI method, taking into account single and double excitations with the addition of the Davidson correction, implemented in the DIRAC [33] program. The dependence of quantum-electrodynamic (QED) corrections to the ground state energy of the OH molecule as a function of the internuclear distance was also investigated. The calculations were performed by the model-QED operator QEDMOD [34] by means of the MRCI method in the basis of the Dirac-Fock-Sturm orbitals (MRCI-DFS) [35–37]. Previously, the MRCI-DFS method was successfully tested in calculations of the electronic structure of the CO [38] and CN molecules [39].

Calculation details

Coupled cluster method

Relativistic calculations of the mass-invariant Born-Oppenheimer (BO) curve and the eigen dipole moment function for the lower $^2\Pi_{\Omega=3/2}$ component of the $X^2\Pi$ electronic ground state of the OH molecule (recall, the ground state of OH has the so-called „reversed“ multiplet) were carried out by the single-reference coupled cluster (CC) method with the inclusion of single, double, and triple cluster amplitudes, and the triple excitations were taken into account both by multiparticle perturbation theory (CCSD(T)) and by the exact nonperturbative method (CCSDT). The Dirac-Hartree-Fock (DHF) approach with the relativistic four-component Dirac−Coulomb Hamiltonian, implemented in the DIRAC program, was used to construct the one-electron basis. Calculations by the coupled cluster method were also performed in the package EXP-T [40], which provides the possibility of fully accounting for threefold cluster amplitudes. The permanent dipole moment was calculated using the finite field method with field strength values ± 0.0001 a. u.

In CC calculations, standard correlation-oriented basis sets of primitive Gaussian functions aug-cc-pVnZ with the cardinal number $n = 5$ and 6 [41]were used. In correlation calculations by the CCSD and CCSD(T) methods, all 9 electrons were explicitly correlated with the inclusion of virtual orbitals with energies up to 300 a. u. An additional calculation with the aug-cc-pV5Z basis showed a contribution from the inclusion of virtual orbitals from 300 to 10000 a. u. to the energy curve at the level of $5\,\mathrm{cm}^{-1}$ and to the dipole moment curve — at the level of 10^{-4} D in the available range of inter-nuclear distances. The correction for the full contribution of the threefold cluster amplitudes relative to their perturbative account was determined as the difference between the results of CCSDT and CCSD(T) calculations on the cc-pVnZ ($n = 5, 6$) bases with a correlation of 7 electrons and taking into account virtual orbitals up to 30 a. u. To obtain the final CCSDT values, the corresponding correction was added to the results of systematic calculations by the CCSD(T) method.

The results of the $E_{\mathrm{corr}}(n)$ correlation energy calculations were extrapolated to the complete basis set (CBS) $E_{\mathrm{corr}}^{\mathrm{CBS}}$ using the following formula with $n = 5, 6$:

$$E_{\mathrm{corr}}(n) = E_{\mathrm{corr}}^{\mathrm{CBS}} + \frac{A}{n^3}. \qquad (1)$$

This formula was also used in extrapolating the values of the permanent dipole moment to the complete basis set. The calculation error due to the incompleteness of the basis set was estimated as the difference between the results corresponding to the extrapolation to CBS and the basis with $n = 6$.

The relativistic corrections to the energy and dipole momenta were determined as the difference between the results of calculations with the Dirac-Coulomb Hamiltonian and the nonrelativistic Schrödinger Hamiltonian obtained using the same basis set. For the most complete account of relativistic effects, the relativistic correction for the interelectron interaction was calculated in the approximation of the Gaunt V^{G} operator:

$$V_{ij}^{\mathrm{G}} = -\frac{(\boldsymbol{\alpha}_i \cdot \boldsymbol{\alpha}_j)}{r_{ij}}. \quad (2)$$

The operator was included in the calculation at the DHF method level using the two-component molecular mean-field Hamiltonian H^{X2Cmmf} [42] and the aug-cc-pV5Z basis. This energy correction was calculated as the difference between the energy with and without the Gaunt interaction included. The magnitude of the spin-orbit splitting was calculated as the difference between the energies of $X^2\Pi_{3/2}$ and $X^2\Pi_{1/2}$ terms obtained using the aug-cc-pV5Z basis.

DIRAC program configuration interaction method

The standard basis set of Gaussian functions aug-cc-pCV5Z was used in the MRCI calculation in the DIRAC program. The four-component Dirac-Coulomb Hamiltonian was taken as the Hamiltonian of the molecular system. In the first step of the calculation, Dirac-Fock orbitals were obtained, and the unpaired electron at the $2p\pi$ orbital was averaged over the four spin orbitals $2p\pi$ and $2p\sigma^*$ to further better reproduce the excited levels. In the next step of MRCI, the configurations formed by all possible rearrangements of all 9 electrons in the 7 lower orbitals were considered in the construction of the reference space. During the construction of the MRCI matrix, single and double excitations from the obtained reference configurations into the space of active and virtual orbitals were taken into account. The choice of the number of virtual orbitals for CI is a nontrivial task, since in the KRCI module of the DIRAC program the diagonalization process of the CI matrix ceases to converge when high energy orbitals are used. By means of numerical experiments it was found that for the OH molecule 190 orbitals can be taken as a virtual basis set, and the procedure of searching for the lower eigenvalues of the CI matrix will converge well.

When performing MRCI calculations with single and double excitations, it may be necessary to take into account the so-called Davidson-type corrections [43], which allow *a posteriori* to partially account for the contribution of three- and fourfold excitations. Although DIRAC has a built-in capability to compute Davidson [44] corrections, unfortunately at the moment the corresponding module of the program does not work properly. Therefore, in this study, an in-house procedure for obtaining Davidson corrections was applied to all calculations. To do this, in addition to the standard calculation it is necessary to carry out a calculation where only the reference configurations of the standard calculation are used as basis determinants, i.e. full-CI in the basis of orbitals from which the reference space of the standard calculation is constructed. Then the Davidson corrections can be obtained by the formula [45]

$$\Delta E = \frac{(N-2)(N-3)}{N(N-1)} \frac{1-\sum_{j\in\mathrm{ref}}|c_j|^2}{\sum_{j\in\mathrm{ref}}|c_j|^2} \times (E_{\text{MRCI-SD}} - E_{\text{Full-CI-ref}}), \quad (3)$$

where $E_{\text{MRCI-SD}}$ and $E_{\text{Full-CI-ref}}$ — the energies obtained in the standard and complementary calculation, respectively, $\sum_{j\in\mathrm{ref}}|c_j|^2$ — the sum of the squares of the coefficients of the reference configurations in the CI decomposition of the standard calculation wave function, N — the number of correlated electrons.

The permanent dipole moment can be calculated using the MRCI approach in two ways. The first way is to calculate the matrix element of the dipole moment operator on CI wave functions. The alternative approach is based on the finite field method and allows for additional consideration of Davidson corrections, so it is considered to be more accurate. However, the accuracy of the calculation of the field derivative of the energy must be carefully controlled. If the dipole moment varies strongly with the internuclear distance or its value is close to zero, the first approach is preferable.

The method of Multi-Reference Configuration Interaction in the basis of the Dirac-Fock-Sturm orbitals

The MRCI-DFS method as applied to two-atomic molecules has been described in detail in [38,39]. In the MRCI-DFS method, the multielectron wave function of a molecule with a certain value of the Ω projection of the total angular momentum onto the internuclear axis is constructed as a linear combination of Slater determinants consisting of one-electron molecular orbitals obtained by solving the two-center Dirac-Fock equations. The molecular orbitals are constructed in the basis of one-center Dirac-Fock-Sturm (DFS) orbitals. The DFS orbitals are constructed separately for each atom during the solution of the DFS equations.

QED corrections to the total energy of the OH molecule were obtained using the model-QED-operator technique [34]. In calculating the QED corrections, the model operator is added to the Hamiltonian in the step of constructing the DFS basis, when solving the DF molecular equations and calculating the CI matrix.

Results and discussion

Potential energy functions

In this paper, potential energy curves of the ground state and some excited states in a wide region of inter-nuclear distances $R \in [0.5, 5.0]$ Å were obtained by means of the MRCI method of the DIRAC program. The Davidson correction was also taken into account by the method described in the previous section. By diagonalizing the CI matrix, the energies of 8 lowest states with $\Omega = 1/2$, 4 lowest states with $\Omega = 3/2$ and 2 states with $\Omega = 5/2$ were calculated. Since some levels with the same value of Ω have quasi-intersections at different points of R_c, the nomenclature of the non-relativistic term of a particular level may vary with distance. Fig. 1 shows the potential energy curves of states corresponding to the first three non-relativistic dissociation limits. The color and shape of the dots are used to indicate the levels to which correspond certain ordinal number and projection of the total angular momentum.

The obtained curves correlate with the following non-relativistic terms: $X^2\Pi$, $A^2\Sigma^+$, $a^4\Sigma^-$, $1^2\Sigma^-$, $1^4\Pi$, $2^2\Pi$ and $B^2\Sigma^+$ for $\Omega = 1/2$; $X^2\Pi$, $a^4\Sigma^-$, $1^4\Pi$ and $1^2\Delta$ for $\Omega = 3/2$; $1^4\Pi$ and $1^2\Delta$ for $\Omega = 5/2$. At the same time, level $1^4\Pi$ includes two close levels with $\Omega = 1/2$: with $\Lambda = 1$ and $\Sigma = -1/2$ and $\Lambda = -1$ and $\Sigma = 3/2$, and also one level each with $\Omega = 3/2$ and $\Omega = 5/2$.

Figure 2 shows the difference between the ground state energy curves of $X^2\Pi_{3/2}$, obtained in this study and the empirical RKR (Rydberg-Klein-Rees) data from [46]. The curves were shifted to zero at the point corresponding to the equilibrium internuclear distance R_e.

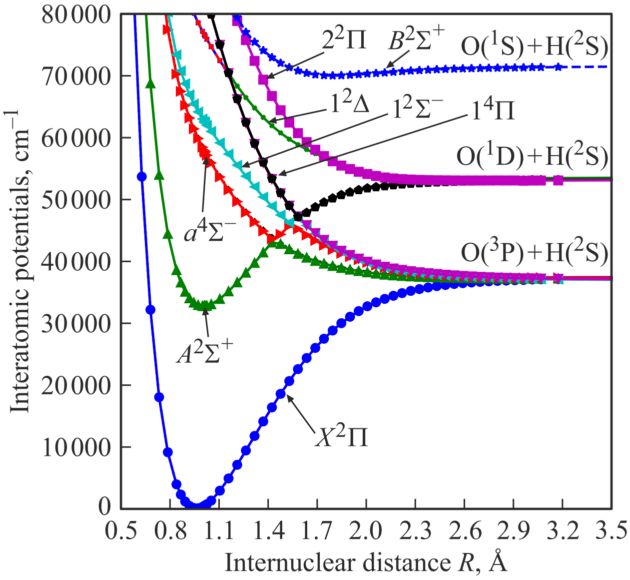

Figure 1. Relativistic potential energy curves of the OH molecule obtained in this work by the MRCI method of the DIRAC program. The curves with a certain color and shape of points correspond to a certain ordinal number of the level in the diagonalization of the CI matrix. Additionally, the figure shows the designations of the non-relativistic terms of the molecule, which can be correlated with these relativistic curves.

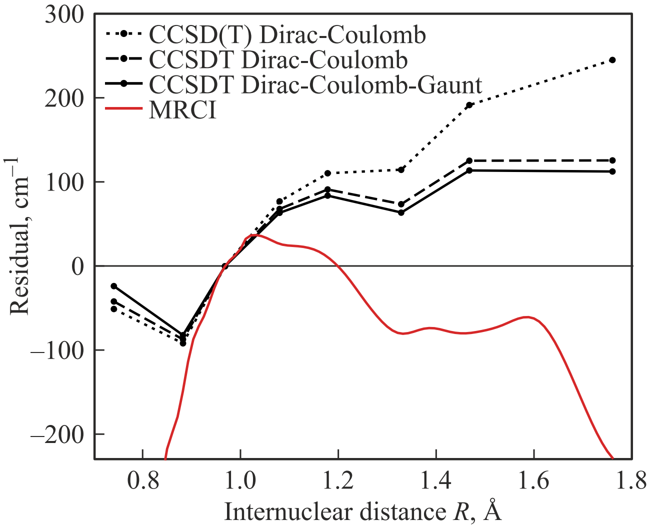

Figure 2. The ground state potential energy $X^2\Pi_{3/2}$ of the OH molecule obtained by the single-reference CC method with various levels of cluster amplitude treatment, both with and without inclusion of the Gaunt interaction. Values obtained by the MRCI method without including the Gaunt are also shown for comparison. The data are presented relative to the empirical RKR potential from the work of [46] and shifted to zero at the point corresponding to the equilibrium internuclear distance.

The single-reference cluster method allows results for internuclear distances up to 1.8 Å. The computational error is determined by the incompleteness of the basis set and is estimated to be 50 cm^{-1}. In the given range of internuclear distances, the difference between the method with full consideration of threefold amplitudes and the semiempirical curve does not exceed 100 cm^{-1}. The MRCI method gives a similar difference for distances from 0.9 to 1.6 Å; for larger distances, the discrepancy with the empirical curve increases sharply. This behavior can be explained by the gradual strengthening of the effect of mixing configurations. Thus, the $\pi^2_{1/2}\pi^1_{3/2}$ configuration, dominating at the equilibrium internuclear distance with a weight of more than 0.9, by 1.8 Å has a weight of about 0.7. A certain improvement in the accuracy of calculations can be achieved by considering higher order excitations, as can be seen in the example of the single-reference method of coupled clusters. The difference from the empirical data in the region 1.8 Å for the CCSD method is about 1800 cm^{-1}, CCSD(T) — 250 cm^{-1}, and for the CCSDT — 100 cm^{-1}. At the same time, for internuclear distances larger than 1.2 Å the accuracy of the method with full consideration of threefold CCSDT amplitudes drops much slower than in the case of the CCSD(T) perturbative approach.

The relativistic correction and the Gaunt interaction contribution to the potential energy curve of the ground state of the molecule are shown in Figs. 3 and 4. It can be seen that the Gaunt contribution at equilibrium

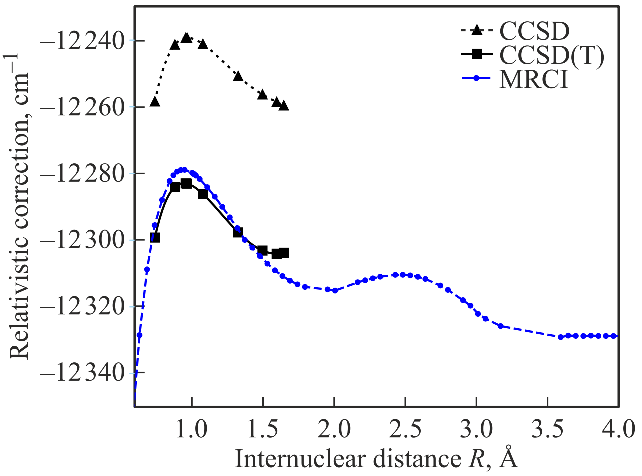

Figure 3. Relativistic correction for the potential energy curves of the ground state of the OH molecule obtained by the CC and MRCI methods in the framework of the Dirac-Coulomb Hamiltonian.

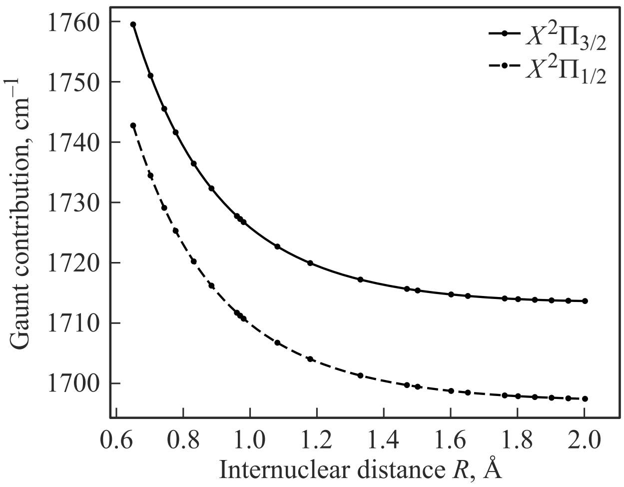

Figure 4. Relativistic correction from the Gaunt contribution to the potential energy curves of the $X^2\Pi_{3/2}$ and $X^2\Pi_{1/2}$ terms of the OH molecule obtained at the level of the DHF method.

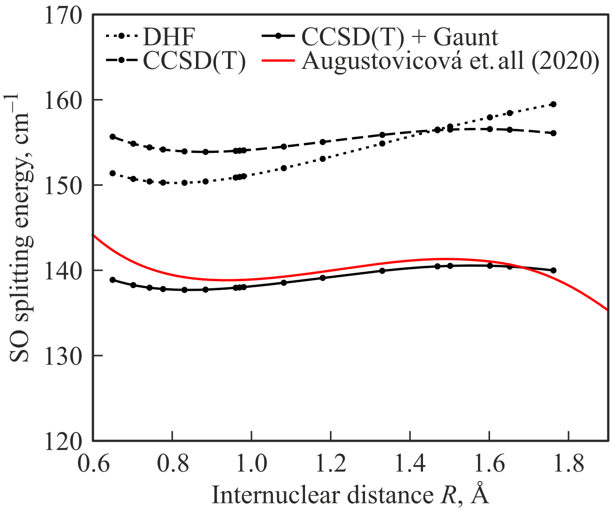

Figure 5. The spin-orbit (SO) splitting of the ground state of $X^2\Pi$ at the level of DHF and CCSD(T) methods and with Gaunt's contribution taken into account. A comparison with a semiempirical function from [20] is given.

Convergence of the equilibrium internuclear distance R_e (Å) of the ground state $X^2\Pi_{3/2}$ of the OH molecule as a function of the completeness of the basis set used, the level of accounting for cluster amplitudes and Gaunt interactions

	CCSD	CCSD(T)	CCSDT
	Dirac-Coulomb		
$n = 4$	0.9670	0.9698	0.9699
$n = 5$	0.9666	0.9694	0.9696
$n = 6$	0.9663	0.9692	0.9694
CBS	0.9662	0.9690	0.9692
	Dirac-Coulomb-Gaunt		
CBS	0.9663	0.9692	0.9694
MRCI [18]	0.9702		
Exp. [47]	0.96966		

distance has a value of about 15 cm^{-1} relative to the atomic limit, and the relativistic contribution is about 50 cm^{-1}. Fig. 5 shows the spin-orbit splitting energy of the ground state of the molecule. Accounting for electron correlations hardly affects the splitting, while the Gaunt interaction causes its significant shift. The splitting itself practically does not change in the given range of internuclear distances and amounts to 138 cm^{-1} at the equilibrium distance.

The table summarizes the results of equilibrium internuclear distance R_e, calculations performed by the single-reference CC coupled cluster method with different levels of cluster amplitude accounting — both with and without the inclusion of Gaunt interaction. The inclusion of Gaunt interaction similar to the full accounting of triple amplitudes compared to their perturbative consideration leads to an increase in the bond length of the molecule by 0.0002 Å. At the same time, extrapolation to an infinite basis set relative to the largest one in use decreases this distance by the same amount. The final value of R_e equal to 0.9694 Å is in good agreement with the experimental value of 0.96966 Å [47]. The equilibrium distance obtained by the MRCI method is 0.9699 Å.

In the framework of the model-QED-operator method by the MRCI-DFS method, the value of the QED corrections to the total electronic energy of the OH molecule as a function of the internuclear distance was calculated. Fig. 6 shows the relative curve of the QED corrections for the distances

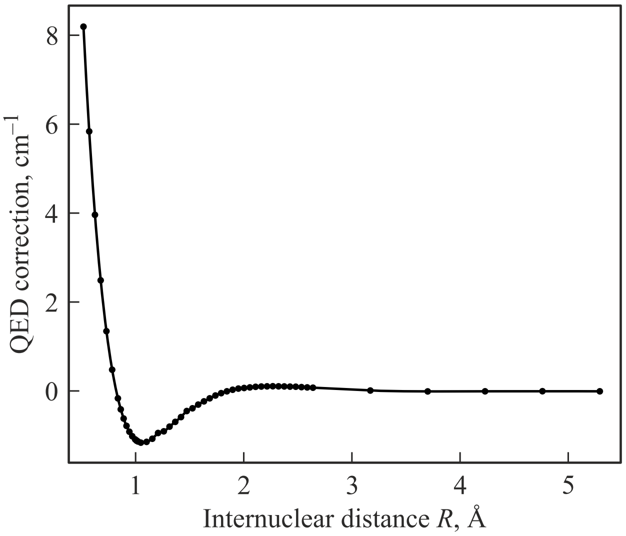

Figure 6. Dependence of the QED corrections to the ground state energy $X^2\Pi_{3/2}$ of the OH molecule on the internuclear distance calculated by the MRCI-DFS method as part of the model-QED operator. The energy value corresponding to the dissociation limit is taken as zero.

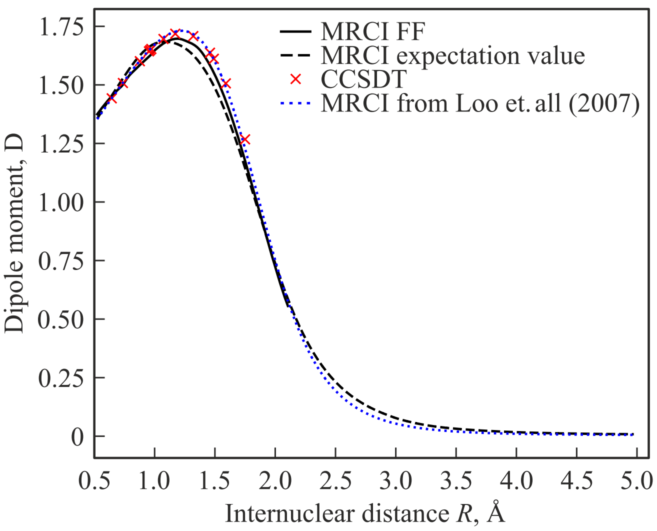

Figure 7. Relativistic permanent dipole moment functions of the ground state $X^2\Pi_{3/2}$ dipole moment of the OH molecule obtained by CCSDT and MRCI methods within the finite field (FF) approximation and by calculating the mean value. The results of the nonrelativistic calculation and the study [18] are given for comparison.

$R \in [0.5, 5.5]$ Åshifted to zero at the dissociation limit. The absolute value of the QED corrections is 1037.7 cm^{-1}. The relative QED curve has a minimum in the vicinity of the R_e point, the depth of which is 1 cm^{-1}. Thus, the effect of QED corrections on the basic molecular constants such as equilibrium internuclear distance and dissociation energy is negligible.

Ground state dipole moment

The ground state permanent dipole moment $X^2\Pi_{3/2}$ of the OH molecule in the range of internuclear distances $R \in [0.5, 5.5]$ Å was calculated by the relativistic MRCI method. Since at distances $R \geq 3.0$ Å the dipole moment asymptotically tends to zero, its value in a wide region of internuclear distances was obtained by averaging the dipole moment operator on the electronic wave functions of the ground state. The eigen dipole moment was also calculated by the coupled cluster method for internuclear distances from 0.7 to 1.8 Å. The contribution of the Gaunt interaction was less than 0.001 D, so it was not taken into account in the final results.

Figure 7 shows the results of the dipole moment function calculation obtained in this paper, and compares it with the nonrelativistic function taken from [18], in which the dipole moment was calculated as the mean value of the corresponding operator (the expectation value) by a similar MRCI method. Figure 7 shows a good agreement of the considered dependences. The difference between the dipole moments obtained by the MRCI method in this study and in [18] is up to 0.1 D. After passing the maximum region, the curve smoothly decreases to zero at distances close to the dissociation limit. Fig. 8 shows a comparison of the difference between the calculated values of the ground state dipole moment and the empirical function proposed in [48]. Furthermore, a comparison with the results of the [49] study, in which the final values were obtained by combining the CCSD(T) calculations near the equilibrium internuclear distance with the results obtained by the MR-ACPF (multi-reference averaged coupled-pair functional) method at larger distances, has been made. As expected, our results using the CCSD(T) method are in good agreement with those of [49], where a similar approach was used. Taking full account of the threefold amplitudes in the calculation improves the accuracy: in the range of internuclear distances from 0.8 to 1.6 Å the deviation does not exceed 0.02 D.

Dipole moments of electron transitions

In this section we provide the results of a relativistic calculation of both spin-allowed and spin-forbidden electronic transitions between the low-lying doublet and quartet states of the OH molecule.

Fig. 9 shows the results of calculating the spin-allowed dipole moment function for the $A^2\Sigma^+_{1/2} - X^2\Pi_{3/2}$ transition in the inter-nuclear distance range $R \in [0.5, 5.5]$ Å performed by the MRCI method using the DIRAC program. To compare, the results of the non-relativistic calculation by the MRCISD method in the program MOLPRO [19], as well as empirical results from [50] are also given. The resulting plot shows good agreement of the calculated data for all considered internuclear distances.

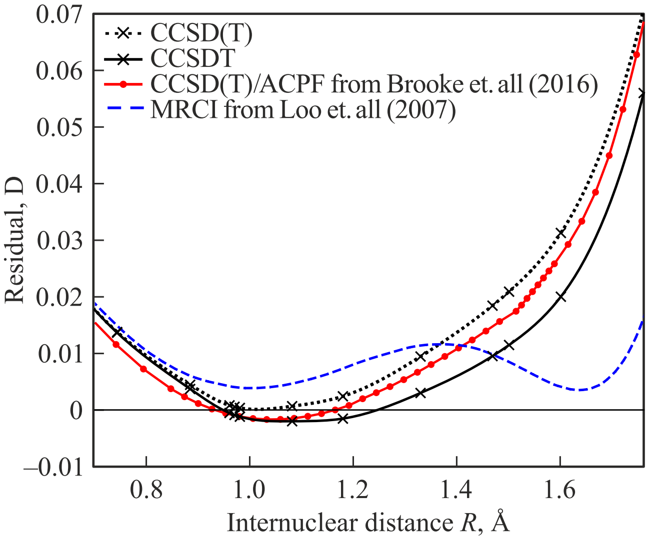

Figure 8. The permanent dipole moment functions of the ground state $X^2\Pi_{3/2}$ of the OH molecule obtained by the CCSD(T) and CCSDT coupled cluster methods. The results of [18,49] are given for comparison. All data are presented relative to the empirical curve proposed in [48].

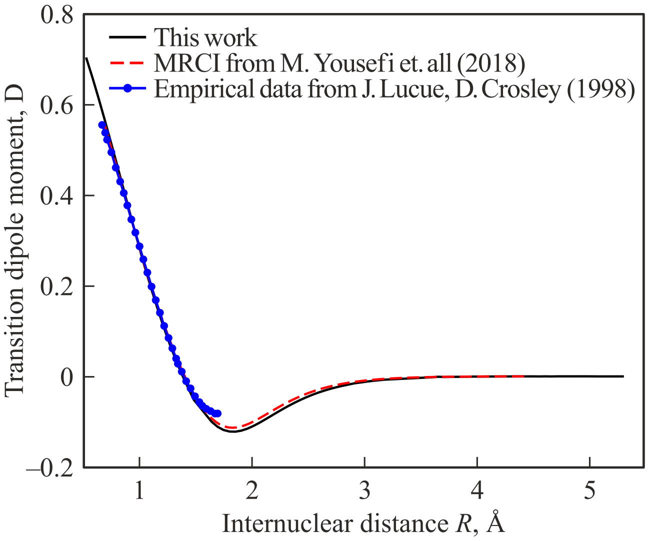

Figure 9. The dipole moment function for the spin-allowed transition $A^2\Sigma_{1/2}$-$X^2\Pi_{3/2}$ obtained by the relativistic MRCI method using the DIRAC program (solid black line), in the nonrelativistic approximation in [19] (dashed red line), and also plotted based on the experimental data (blue line and circles).

Fig. 10 shows the relativistic dipole moment function of the spin-allowed transition $1^2\Sigma^-_{1/2} - X^2\Pi_{3/2}$ in the shortened interval $R \in [0.8, 2.0]$ Å. To estimate the accuracy of the obtained results, we additionally present the nonrelativistic function calculated earlier by the analogous MRCI method in [51]. Visual comparison of the presented functions demonstrates in general a reasonable agreement.

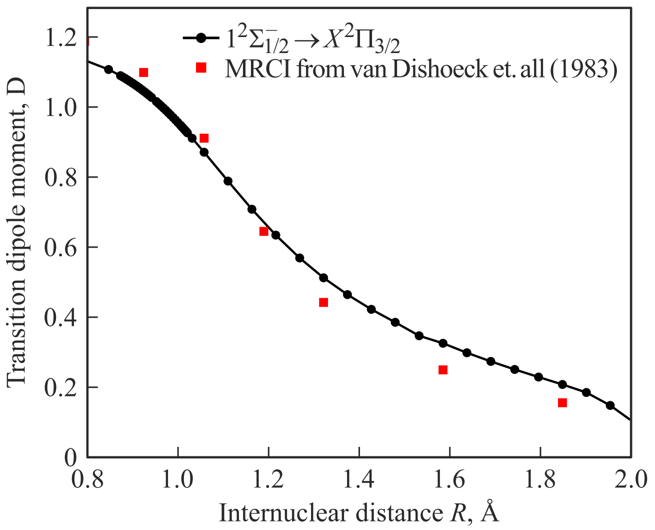

Figure 10. The relativistic function for the spin-allowed dipole moment of the $1^2\Sigma^-_{1/2} - X^2\Pi_{3/2}$ transition obtained by the MRCI method using the DIRAC program, compared with its nonrelativistic counterpart from [51].

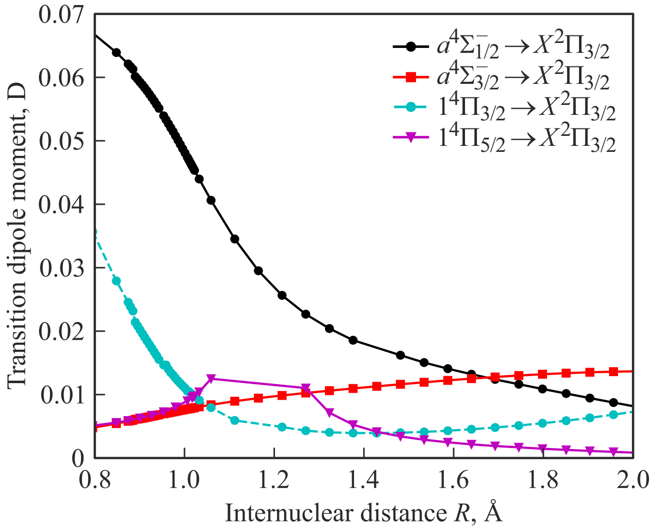

Figure 11. Relativistic dipole moment functions for the quartet-doublet transitions $a^4\Sigma^-_{1/2;3/2} - X^2\Pi_{3/2}$ and $1^4\Pi_{3/2;5/2} - X^2\Pi_{3/2}$ calculated by the MRCI method using the DIRAC program.

Fig. 11 shows the relativistic dipole moment functions for the quartet-doublet transitions $a^4\Sigma^-_{1/2;3/2} - X^2\Pi_{3/2}$ and $1^4\Pi_{3/2;5/2} - X^2\Pi_{3/2}$ obtained using the MRCI method of the DIRAC program over the interval $R \in [0.8, 2.0]$ Å. As one would expect, the absolute magnitude of spin-forbidden transitions was an order of magnitude smaller than the magnitude of spin-allowed transitions. It should be noted that the dipole moment of the transition $1^4\Pi_{5/2} - X^2\Pi_{3/2}$ behaves in a step-wise manner in the region of $R = 1.1$ Å since in this region the term $1^4\Pi_{5/2}$ has a quasi-intersection with the term $1^2\Delta_{5/2}$.

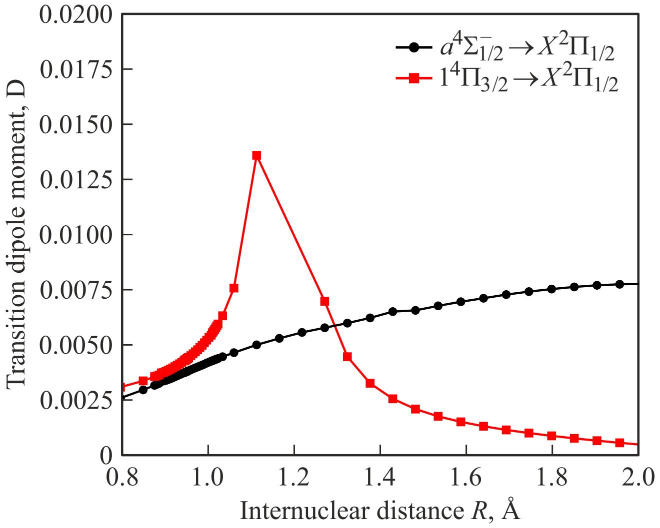

Figure 12. Relativistic dipole moment functions for the quartet-doublet transitions $a^4\Sigma^-_{1/2} \to X^2\Pi_{1/2}$ and $1^4\Pi_{3/2} \to X^2\Pi_{1/2}$calculated by the MRCI method using the DIRAC program.

Figure 12 shows the dipole moments of the $X^2\Pi_{1/2}$state transitions: $a^4\Sigma^-_{1/2} \to X^2\Pi_{1/2}$ and $1^4\Pi_{3/2} \to X^2\Pi_{1/2}$. In this plot, the dipole moment of the $1^4\Pi_{3/2} - X^2\Pi_{1/2}$ transition exhibits similar behavior to the $1^4\Pi_{5/2} - X^2\Pi_{3/2}$ transition in Fig. 11. At the crossing point of the quasi-intersection of the quartet term $1^4\Pi_{3/2}$ with the doublet $1^2\Delta_{3/2}$ the dipole moment curve of $1^4\Pi_{3/2} - X^2\Pi_{1/2}$ has a jump similar to the jump of the dipole moment function of the $1^4\Pi_{5/2} - X^2\Pi_{3/2}$ transition.

Conclusion

In this paper, the low-lying states of the OH molecule over a wide range of internuclear distances were investigated using the relativistic MRCI and CC methods of the DIRAC program, as well as the MRCI-DFS method. Potential energy curves for states with $\Omega = 1/2$, $\Omega = 3/2$ and $\Omega = 5/2$ corresponding to the pure Hund's coupling case „**c**" were calculated by the MRCI approach. These states are formed from the $X^2\Pi$ states, $A^2\Sigma^+$, $a^4\Sigma^-$, $1^2\Sigma^-$, $1^4\Pi$, $1^2\Delta$, $2^2\Pi$ and $B^2\Sigma^+$, which correspond to the case of Hund coupling „**a**" by spin-orbit interaction. Near the minimum of the potential curve of the $X^2\Pi_{3/2}$ ground state, the electronic structure of the OH molecule was also calculated using the single-reference CC method, yielding a value of the equilibrium bond length close to the experimental value.

An additional calculation of the relativistic correction for the ground state $X^2\Pi_{3/2}$ of the OH molecule was carried out using the MRCI and CC methods. The data obtained by the MRCI and CC methods are in good agreement with each other. The absolute value of the correction was about 12300 cm^{-1} with a relative value of about 50 cm^{-1} near the minimum of the potential curve compared to the dissociation limit. In addition, the contribution of the Gaunt interaction to the spin-orbit splitting of the ground state of the OH molecule was investigated. It turned out that the Gaunt interaction is essential for an accurate determination of the spin-orbit splitting. The dependence of the spin-orbit splitting on the internuclear distance obtained by the CCSD(T) method shows a high degree of agreement with the semiempirical curve. Overall, the present results emphasize the importance of relativistic calculations in the study of the spectroscopic properties of even such a light molecule as OH.

For the $X^2\Pi_{3/2}$ state in the framework of the model-QED operator by the MRCI-DFS method, the value of the QED of corrections to the electronic energy of the molecule as a function of the internuclear distance was obtained. The absolute value of the QED corrections was about 1037 cm^{-1}, and the QED function has a minimum near R_e with a depth of about 1 cm^{-1}. Thus, accounting for QED interactions has negligible effect on the value of the molecular constants of the OH molecule.

A relativistic calculation of the $X^2\Pi_{3/2}$ state permanent dipole moment function in the region was carried out using the MRCI method. In the vicinity of the potential energy minimum, additional calculations were carried out using the CC method in conjunction with the finite field approach. Comparison with previous theoretical studies and available empirical data showed a high level of agreement. In particular, at the equilibrium internuclear distance R_e the dipole moment obtained via the CC method deviates from the experimental value by less than one hundredth of a debye.

For the first time the dipole moment functions for both spin-allowed and spin-forbidden transitions of low-lying excited states of the OH molecule to the ground electronic state were calculated using the relativistic MRCI method. The dipole moment functions obtained for the spin-allowed $A^2\Sigma_{1/2} - X^2\Pi_{3/2}$ and spin-forbidden $1^2\Sigma^-_{1/2} - X^2\Pi_{3/2}$ transitions were compared with data available in the literature. The observed consistency between the relativistic and nonrelativistic results supports the overall reliability of the present calculations.

Funding

The study was supported by the Russian Science Foundation (interdisciplinary Grant No. 22-62-00004, https://rscf.ru/project/22-62-00004/). The calculations were performed using the heterogeneous computing platform HybriLIT (LIT, JINR) [52].

Conflict of interest

The authors declare that they have no conflict of interest.

References

[1] I.A.B. Meinel. Astrophys. J., **111**, 555 (1950).
[2] A.B. Meinel. Astrophys. J., **111**, 207 (1950).
[3] P.C. Cosby, T.G. Slanger. Canadian Journal of Physics, **85** (2), 77 (2007).
[4] R.G. Prinn, R.F. Weiss, B.R. Miller, J. Huang, F.N. Alyea, D.M. Cunnold, P.J. Fraser, D.E. Hartley, P.G. Simmonds. Science, **269** (5221), 187 (1995).
[5] J. Lelieveld, F.J. Dentener, W. Peters, M.C. Krol. Atmospheric Chemistry and Physics, **4** (9/10), 2337 (2004).
[6] T.B. Settersten, R.L. Farrow, J.A. Gray. Chemical Physics Letters, **369** (5), 584 (2003).
[7] N. Grevesse, A.J. Sauval, E.F. van Dishoeck. Astronomy and Astrophysics, **141** (1), 10 (1984).
[8] J. Meléndez, B. Barbuy. The Astrophysical Journal, **575** (1), 474 (2002).
[9] Asplund, M., Grevesse, N., Sauval, A. J., Allende Prieto, C., Kiselman, D.. AA, **435** (1), 339 (2005).
[10] B.J. Robinson, R.X. McGee. Annual Review of Astronomy and Astrophysics, **5** (Volume 5, 1967), 183 (1967).
[11] J.R. Goicoechea, J. Cernicharo. The Astrophysical Journal, **576** (1), L77 (2002).
[12] Piccioni, G., Drossart, P., Zasova, L., Migliorini, A., Gérard, J.-C., Mills, F. P., Shakun, A., García Muñnoz, A., Ignatiev, N., Grassi, D., Cottini, V., Taylor, F. W., Erard, S., the VIRTIS-Venus Express Technical Team. A&A, **483** (3), L29 (2008).
[13] P.E. Cade, W.M. Huo. The Journal of Chemical Physics, **47** (2), 614 (1967).
[14] W.J. Stevens, G. Das, A.C. Wahl, M. Krauss, D. Neumann. The Journal of Chemical Physics, **61** (9), 3686 (1974).
[15] W. Meyer, P. Rosmus. The Journal of Chemical Physics, **63** (6), 2356 (1975).
[16] J. Charles W. Bauschlicher, S.R. Langhoff. The Journal of Chemical Physics, **87** (8), 4665 (1987).
[17] S.R. Langhoff, J. Charles W. Bauschlicher, P.R. Taylor. The Journal of Chemical Physics, **91** (10), 5953 (1989).
[18] M.P.J. van der Loo, G.C. Groenenboom. The Journal of Chemical Physics, **126** (11), 114314 (2007).
[19] M. Yousefi, P.F. Bernath, J. Hodges, T. Masseron. JQSRT, **217**, 416 (2018).
[20] L.D. Augustovičová, V. Špirko. Journal of Quantitative Spectroscopy and Radiative Transfer, **254**, 107211 (2020).
[21] Y.G. Borkov, O.N. Sulakshina, S.V. Kozlov, T.I. Velichko. Optics and Spectroscopy (English translation of Optika i Spektroskopiya), **128** (12), 1921 (2020).
[22] S.V. Kozlov, E.A. Pazyuk. Optics and Spectroscopy (English translation of Optika i Spektroskopiya), **130** (12), 1517 (2022).
[23] H. Michels, F. Harris. Chemical Physics Letters, **3** (6), 441 (1969).
[24] I. Easson, M.H.L. Pryce. Canadian Journal of Physics, **51** (5), 518 (1973).
[25] D.R. Yarkony. The Journal of Chemical Physics, **97** (3), 1838 (1992).
[26] A. Varandas, A. Voronin. Chemical Physics, **194** (1), 91 (1995).
[27] G. Parlant, D.R. Yarkony. The Journal of Chemical Physics, **110** (1), 363 (1999).
[28] Y. Li, P.Y. Zhang. Journal of Theoretical and Computational Chemistry, **10** (06), 747 (2011).
[29] X. Qin, S.D. Zhang. Journal of the Korean Physical Society, **65** (12), 2017 (2014).
[30] G.B. Mitev, J. Tennyson, S.N. Yurchenko. The Journal of Chemical Physics, **160** (14), 144110 (2024).
[31] S.V. Kozlov, E.A. Pazyuk, A.V. Stolyarov. Russian Journal of Physical Chemistry A, **98** (5), 89 (2024).
[32] G.B. Mitev, J. Tennyson, S.N. Yurchenko. The Journal of Chemical Physics, **160** (14), 144110 (2024).
[33] DIRAC, a relativistic ab initio electronic structure program, Release DIRAC19 (2019), written by A.S.P. Gomes, T. Saue, L. Visscher, H.J.Aa. Jensen, and R. Bast, with contributions from I.A. Aucar, V. Bakken, K.G. Dyall, S. Dubillard, U. Ekström, E. Eliav, T. Enevoldsen, E. Faßhauer, T. Fleig, O. Fossgaard, L. Halbert, E.D. Hedegård, B. Heimlich-Paris, T. Helgaker, J. Henriksson, M. Iliaš, Ch.R. Jacob, S. Knecht, S. Komorovský, O. Kullie, J.K. Lærdahl, C.V. Larsen, Y.S. Lee, H.S. Nataraj, M.K. Nayak, P. Norman, G. Olejniczak, J. Olsen, J.M.H. Olsen, Y.C. Park, J.K. Pedersen, M. Pernpointner, R. di Remigio, K. Ruud, P. Sa lek, B. Schimmelpfennig, B. Senjean, A. Shee, J. Sikkema, A.J. Thorvaldsen, J. Thyssen, J. van Stralen, M.L. Vidal, S. Villaume, O. Visser, T. Winther, and S. Yamamoto (available at http://dx.doi.org/10.5281/zenodo.3572669, see also http://www.diracprogram.org).
[34] V.M. Shabaev, I.I. Tupitsyn, V.A. Yerokhin. Phys. Rev. A, **88** (1), 012513 (2013).
[35] I.I. Tupitsyn, A.V. Loginov, Opt. and spektr.,., **94** (3), 357 (2003) [Opt. Spectrosc., **94** (3), 319 (2003)].
[36] I.I. Tupitsyn, V.M. Shabaev, J.R. Crespo López-Urrutia, I. Draganić, R. Soria Orts, J. Ullrich. Phys. Rev. A, **68** (2), 022511 (2003).
[37] I.I. Tupitsyn, A.V. Volotka, D.A. Glazov, V.M. Shabaev, G. Plunien, J.R. Crespo López-Urrutia, A. Lapierre, J. Ullrich. Phys. Rev. A, **72** (6), 062503 (2005).
[38] N.K. Dulaev, I.I. Tupitsyn, D.P. Usov, A.M. Ryzhkov, V.M. Shabaev. Opt. Spectrosc., **131** (8), 1033 (2023). (in Russian)
[39] N.K. Dulaev, I.I. Tupitsyn, D.P. Usov, Y.S. Kozhedub, A.M. Ryzhkov, I.M. Savelyev, V.M. Shabaev. Opt. and spektr., **131** (12), 1618 (2023).
[40] A.V. Oleynichenko, A. Zaitsevskii, E. Eliav Towards high performance relativistic electronic structure modelling: The exp-t program package in *Russian Supercomputing Days*, pp. 375–386, Springer, 2020.
[41] A.K. Wilson, T. Van Mourik, T.H. Dunning Jr. Journal of Molecular Structure: THEOCHEM, **388**, 339 (1996).
[42] J. Sikkema, L. Visscher, T. Saue, M. Iliaš. The Journal of chemical physics, **131** (12), 124116 (2009).
[43] P.G. Szalay, T. Müller, G. Gidofalvi, H. Lischka, R. Shepard. Chemical Reviews, **112** (1), 108 (2012).
[44] https://www.diracprogram.org/doc/release-14/tutorials/relci_q_corrections/q_corrections.html.
[45] L. Meissner. Chemical Physics Letters, **146** (3), 204 (1988).
[46] R.J. Fallon, I. Tobias, J.T. Vanderslice. The Journal of Chemical Physics, **34** (1), 167 (1961).
[47] K. Huber Molecular spectra and molecular structure: IV. Constants of diatomic molecules. Springer Science & Business Media, 2013.
[48] D.D. Nelson Jr, A. Schiffman, D.J. Nesbitt, J.J. Orlando, J.B. Burkholder. The Journal of chemical physics, **93** (10), 7003 (1990).

[49] J.S. Brooke, P.F. Bernath, C.M. Western, C. Sneden, M. Afşar, G. Li, I.E. Gordon. JQSRT, **168**, 142 (2016).

[50] J. Luque, D.R. Crosley. The Journal of Chemical Physics, **109** (2), 439 (1998).

[51] E.F. van Dishoeck, S.R. Langhoff, A. Dalgarno. The Journal of Chemical Physics, **78** (7), 4552 (1983).

[52] G. Adam, M. Bashashin, D. Belyakov, M. Kirakosyan, M. Matveev, D. Podgainy, T. Sapozhnikova, O. Streltsova, S. Torosyan, M. Vala et al. T *Selected Papers of the 8th International Conference „Distributed Computing and Gridtechnologies in Science and Education“* (GRID 2018), pp. 638–644, 2018.

Translated by J.Savelyeva